







RESEARCH ARTICLE | OCTOBER 31 2024

Superconducting (Ba,K)Fe₂As₂ epitaxial films on single and bicrystal SrTiO₃ substrates

Dongyi Qin ; Zimeng Guo ; Chiara Tarantini ; Satoshi Hata ; Michio Naito ; Akiyasu Yamamoto 



Appl. Phys. Lett. 125, 182601 (2024)

<https://doi.org/10.1063/5.0233645>

 CHORUS



View Online



Export Citation

Articles You May Be Interested In

Evidence for composition variations and impurity segregation at grain boundaries in high current-density polycrystalline K- and Co-doped BaFe₂As₂ superconductors

Appl. Phys. Lett. (October 2014)

Pressure-induced shift of T_c and structural transition in “122” type pnictide superconductor

Ca_{0.34}Na_{0.66}Fe₂As₂

AIP Advances (July 2016)

Josephson junction in cobalt-doped BaFe₂As₂ epitaxial thin films on (La, Sr)(Al, Ta)O₃ bicrystal substrates

Appl. Phys. Lett. (April 2010)



Applied Physics Letters

Special Topics Open for Submissions

[Learn More](#)

Superconducting (Ba,K)Fe₂As₂ epitaxial films on single and bicrystal SrTiO₃ substrates

Cite as: Appl. Phys. Lett. **125**, 182601 (2024); doi: [10.1063/5.0233645](https://doi.org/10.1063/5.0233645)

Submitted: 16 August 2024 · Accepted: 21 October 2024 ·

Published Online: 31 October 2024



View Online



Export Citation



CrossMark

Dongyi Qin,^{1,a)} Zimeng Guo,² Chiara Tarantini,³ Satoshi Hata,^{2,4,5} Michio Naito,^{1,5} and Akiyasu Yamamoto^{1,5}

AFFILIATIONS

¹Department of Applied Physics, Tokyo University of Agriculture and Technology, Koganei, Tokyo 184-8588, Japan

²Faculty of Engineering Sciences, Kyushu University, Kasuga, Fukuoka 816-8580, Japan

³Applied Superconductivity Center, National High Magnetic Field Laboratory, Florida State University, Tallahassee, Florida 32310, USA

⁴The Ultramicroscopy Research Center, Kyushu University, 744 Motooka, Nishi, Fukuoka 819-0395, Japan

⁵JST CREST, Kawaguchi, Saitama 332-0012, Japan

^{a)} Author to whom correspondence should be addressed: dongyiqin22@gmail.com

ABSTRACT

The realization of single crystal and bicrystal films of superconducting materials is of great interest because they allow the investigation of the intragrain performance as well as the understanding of potential limitations in the grain boundary transparency. For many years, the realization of a high-quality (Ba,K)Fe₂As₂ film has been challenging. Here, the realization of (Ba,K)Fe₂As₂ epitaxial thin films on single crystal SrTiO₃(001) and [001]-tilt-type SrTiO₃ bicrystal substrates with high superconducting properties is demonstrated. The epitaxial growth of (Ba,K)Fe₂As₂ was enabled by implementing an undoped BaFe₂As₂ buffer layer between the SrTiO₃ substrate and (Ba,K)Fe₂As₂ film. The film exhibits a high T_c of 38.0 K and an extremely high J_c of 14.3 MA/cm² at 4.2 K. Artificial grain boundaries of (Ba,K)Fe₂As₂ were also successfully achieved on bicrystals with misorientation angles up to 36.8° by the same preparation methods. The artificial grain boundaries exhibited an identical T_c of 38.0 K and an excellent transfer of the grain orientation from the bicrystal substrates with high crystallinity comparable to that of the high-quality Ba(Fe,Co)₂As₂ films. This enables the investigation of the intrinsic (Ba,K)Fe₂As₂ grain boundary nature, which will clarify its potential for superconducting applications, like Josephson junctions, wires, and magnets.

Published under an exclusive license by AIP Publishing. <https://doi.org/10.1063/5.0233645>

Fe-based superconductors¹ (FBSS) are promising materials for practical applications that require high magnetic fields such as medical magnetic resonance imaging or fusion reactors.² Among them, (Ba,K)Fe₂As₂ is one of the most extensively studied materials owing to its high superconducting properties; namely critical temperature (T_c) of 38 K,^{3,4} upper critical field up to 90 T,⁵ critical current density (J_c) over 10 MA/cm²,^{6,7} and nearly isotropic electromagnetic property.⁸ These features allow (Ba,K)Fe₂As₂ to be applied as polycrystalline wires and bulks with low-cost fabrication. However, polycrystal applications cannot be achieved without finely tuned grain boundaries as they limit the supercurrent to flow globally. At grain boundaries, supercurrent is either limited by weak-link issues that occur by high-angle misorientation between the neighboring grains or contamination such as impurity or chemical inhomogeneity. The improvement of the transport J_c in (Ba,K)Fe₂As₂ polycrystalline wires has been achieved by attempting various fabrication methods to obtain optimal grain size and grain texture.^{9–13} So far, (Ba,K)Fe₂As₂ has proven its potential in wires reaching

$J_c = 1.6 \times 10^5$ A/cm² at 4.2 K and 10 T,¹² and trapped magnetic field of 2.83 T in superconducting permanent magnets.¹⁴ To further enhance its performance for practical applications, an understanding of the nature of grain boundary is important.

Experiments using artificial grain boundaries (AGBs) are a clear-cut method for investigating the nature of grain boundaries. For the past decades, grain boundary properties of FBSSs have been investigated and reported in Ba(Fe,Co)₂As₂,^{15–17} BaFe₂(As,P)₂,¹⁸ NdFeAs(O,F),¹⁹ and Fe(Se,Te)²⁰ using epitaxial thin films prepared on bicrystal substrates. Despite the high interest, AGBs of (Ba,K)Fe₂As₂ have not been realized due to the difficulty in preparing epitaxial thin films containing highly volatile potassium. Recently, we have reported the (Ba,K)Fe₂As₂ epitaxial thin film achieved by low-temperature growth (~400 °C) and the use of proper substrates and buffer layers.^{21,22} More recently, (Ba,K)Fe₂As₂ epitaxial thin films were prepared on [001]-tilt-type MgO bicrystal substrates with misorientation angles (θ_{GBS}) up to 24°, and their transport properties were investigated.²³ The films

prepared on MgO bicrystal substrates revealed a high grain boundary performance ($J_c > 0.1 \text{ MA/cm}^2$ across AGB with $\theta_{\text{GB}} = 24^\circ$ at 28 K, self-field), which surpasses other FBSs reported so far. In order to observe high-angle grain boundary characteristics of $(\text{Ba,K})\text{Fe}_2\text{As}_2$ film growth on bicrystal substrates with high θ_{GBs} is required. $\text{SrTiO}_3(001)$ substrates are one of the commonly used materials for film growths and are available in the form of bicrystal with high θ_{GBs} up to 36.8° . The use of $\text{SrTiO}_3(001)$ substrates is also advantageous in both terms of lattice matching and its constituent element containing divalent alkaline-earth elements. Indeed, previous reports have proven that the use of SrTiO_3 enables the growth of high-crystallinity epitaxial thin films of $\text{Ba}(\text{Fe,Co})_2\text{As}_2$.^{16,24}

Here, we report the growth of $(\text{Ba,K})\text{Fe}_2\text{As}_2$ epitaxial thin films grown on single crystal $\text{SrTiO}_3(001)$ substrates and [001]-tilt-type SrTiO_3 bicrystal substrates. The epitaxial growth was enabled by implementing a BaFe_2As_2 buffer layer between the SrTiO_3 substrate and $(\text{Ba,K})\text{Fe}_2\text{As}_2$ film. The film exhibits a high T_c of 38.0 K and a J_c exceeding 10 MA/cm^2 , indicating the high quality of the film. The films prepared on [001]-tilt-type SrTiO_3 bicrystal substrates with their θ_{GBs} up to 36.8° exhibit high crystallinity with excellent transfer of the grain orientation from the bicrystal substrates.

Growth of $(\text{Ba,K})\text{Fe}_2\text{As}_2$ epitaxial thin films was performed on $\text{SrTiO}_3(001)$ substrates using a custom-designed molecular beam epitaxy (MBE) system with a base pressure of $1.0 \times 10^{-7} \text{ Pa}$. The MBE system is equipped with electron impact emission spectrometry and atomic absorption spectrometry for precise control of the evaporating flux of the elements. The detailed deposition processes are described in previous reports.^{21,22,25} $\text{SrTiO}_3(001)$ substrates were used because the a -axis length of SrTiO_3 (3.905 \AA) matches well with that of $(\text{Ba,K})\text{Fe}_2\text{As}_2$ ($3.842\text{--}3.962 \text{ \AA}$)²⁶ and are commercially available in the form of bicrystal with high θ_{GBs} up to 36.8° (Furuuchi Chemical Corporation). Many studies have reported that obtaining ideal TiO_2 termination by pretreatments leads to an improved crystallinity of the films,^{27,28} but in this study, as-received SrTiO_3 substrates were used because no significant difference was observed (see the [supplementary material](#), Fig. S1). Since $(\text{Ba,K})\text{Fe}_2\text{As}_2$ films grown directly on $\text{SrTiO}_3(001)$ substrates show no $(\text{Ba,K})\text{Fe}_2\text{As}_2$ peaks (shown in [supplementary material](#), Fig. S2), a BaFe_2As_2 buffer layer was first deposited on the substrate as previously reported.²² The BaFe_2As_2 layer was grown at a high temperature of 600°C and $(\text{Ba,K})\text{Fe}_2\text{As}_2$ was grown at a low temperature of 400°C to prevent re-evaporation of K. The K composition of the $(\text{Ba,K})\text{Fe}_2\text{As}_2$ film was aimed at the optimal composition of $\text{Ba}_{0.6}\text{K}_{0.4}\text{Fe}_2\text{As}_2$. The BaFe_2As_2 buffer layer was deposited at an evaporation rate of $\sim 1 \text{ \AA/s}$ for 3.5 min, yielding a thickness of $\sim 20 \text{ nm}$, and the $(\text{Ba,K})\text{Fe}_2\text{As}_2$ layer was deposited at an evaporation rate of $\sim 1.5 \text{ \AA/s}$ for 10 min, yielding a thickness of $\sim 90 \text{ nm}$. The total pressure during the deposition was $\sim 1.0 \times 10^{-5} \text{ Pa}$. Films were *in situ* coated with CaF_2 on top of the $(\text{Ba,K})\text{Fe}_2\text{As}_2$ at room temperature to further enhance the stability in the air. The resultant films were stable in air and did not degrade upon exposure to air for at least 24 h regardless of the CaF_2 protecting layers.

The crystal structure of the films was evaluated with *in situ* reflection high-energy electron diffraction (RHEED) with an acceleration voltage of 17.6 kV, x-ray diffraction (XRD) using a four-cycle (2θ , ω , χ , ϕ) diffractometer with $\text{CuK}\alpha$ radiation, and cross-sectional transmission electron microscopy (TEM). The axis lengths of the film were estimated using Nelson–Riley extrapolation. a -axis length was

evaluated by the diffraction peaks from the off-axis (103) and (206) planes (see the [supplementary material](#), Fig. S3). The cross-sectional samples for TEM observation were prepared by a focused ion beam in a scanning electron microscope, Helios Hydra CX (Thermo Fisher Scientific). The high-resolution scanning transmission electron microscopy (STEM) images and elemental analysis were obtained by Titan G2 Cubed 60-300 (Thermo Fisher Scientific), which was equipped with bright-field (BF), high-angle annular dark-field (HAADF), and energy-dispersive x-ray spectroscopy detectors. These STEM analyses were operated at an acceleration voltage of 300 kV. In-plane resistivity measurement was conducted with a standard four-probe method with four pins pressed against the film surface to realize electrical conduction. The resistivity of the films was calculated with the total thickness of the $(\text{Ba,K})\text{Fe}_2\text{As}_2/\text{BaFe}_2\text{As}_2$ bilayer. The thickness values of the films were assumed to be 20 and 100 nm for the BaFe_2As_2 buffer layer and $(\text{Ba,K})\text{Fe}_2\text{As}_2$ layer, respectively, which are the typical thicknesses for the same growth condition. T_c values were defined as the temperature at which the resistivity dropped to 90% of its normal-state resistivity above transition ($T_c^{0.9}$), and transition width ΔT_c was defined by the difference of $T_c^{0.9}$ and $T_c^{0.1}$ (the temperature at which the resistivity dropped to 10% of its normal-state resistivity above transition). Magnetization measurements were performed using a superconducting quantum interference device (SQUID) on a rectangular slab with a dimension of $1.65 \times 1.89 \text{ mm}^2 \times \sim 100 \text{ nm}$. J_c was estimated from the magnetization hysteresis loop with Bean critical state model.²⁹

Figure 1(a) shows the out-of-plane XRD pattern of the $(\text{Ba,K})\text{Fe}_2\text{As}_2$ film grown on $\text{SrTiO}_3(001)$ substrate with a 20-nm-thick BaFe_2As_2 buffer layer. Sharp (002 l) peaks confirm that the film has a strong c -axis orientation. Split in the (002 l) peaks was observed in peaks with a higher angle than (004) peaks. The double peaks are attributed to the diffractions from the $(\text{Ba,K})\text{Fe}_2\text{As}_2$ layer at a lower angle and the BaFe_2As_2 layer at a higher angle, indicating the difference in c -axis length having different K concentrations. The difference in the intensity of the peak is consistent with the thickness of each layer. This suggests that two layers exist independently and that there is no apparent elemental diffusion from or into the BaFe_2As_2 buffer layer. Figure 1(b) shows the rocking curve for the (004) reflection of $(\text{Ba,K})\text{Fe}_2\text{As}_2$ with a full width at half maximum (FWHM) of $\Delta\omega_{004} = 0.70^\circ$. The c -axis length and a -axis length of $(\text{Ba,K})\text{Fe}_2\text{As}_2$ layer are estimated to be 13.282 and 3.931 \AA respectively. Compared with $\text{Ba}_{0.6}\text{K}_{0.4}\text{Fe}_2\text{As}_2$ bulks with axis lengths of (a , c) = (3.912, 13.335) (\AA),^{3,26} the film grown on SrTiO_3 substrates has a long a -axis and a short c -axis. In-plane alignment was determined by ϕ -scan around (103) reflection, as shown in Fig. 1(c). The film shows sharp peaks ($\Delta\phi_{103} = 0.86^\circ$) with a fourfold symmetry, reflecting the tetragonal structure of the $(\text{Ba,K})\text{Fe}_2\text{As}_2$. Figures 1(d) and 1(e) show the RHEED patterns of the BaFe_2As_2 buffer layer and $(\text{Ba,K})\text{Fe}_2\text{As}_2$ layer, respectively. Both pictures were taken during the deposition with an electron beam incidence parallel to SrTiO_3 [100] azimuth. The RHEED pattern of the BaFe_2As_2 shows a streak pattern, whereas the $(\text{Ba,K})\text{Fe}_2\text{As}_2$ film exhibits streaky spots. The streaky spots can be interpreted as a rough surface due to the low-temperature growth resulting in a low adatom diffusion. Both pictures resemble the RHEED patterns observed for BaFe_2As_2 and $(\text{Ba,K})\text{Fe}_2\text{As}_2$ film deposited on $\text{CaF}_2(001)$ substrates.²¹ The detailed RHEED patterns during the deposition are shown in the [supplementary material](#) (Fig. S4). The results of XRD analysis and

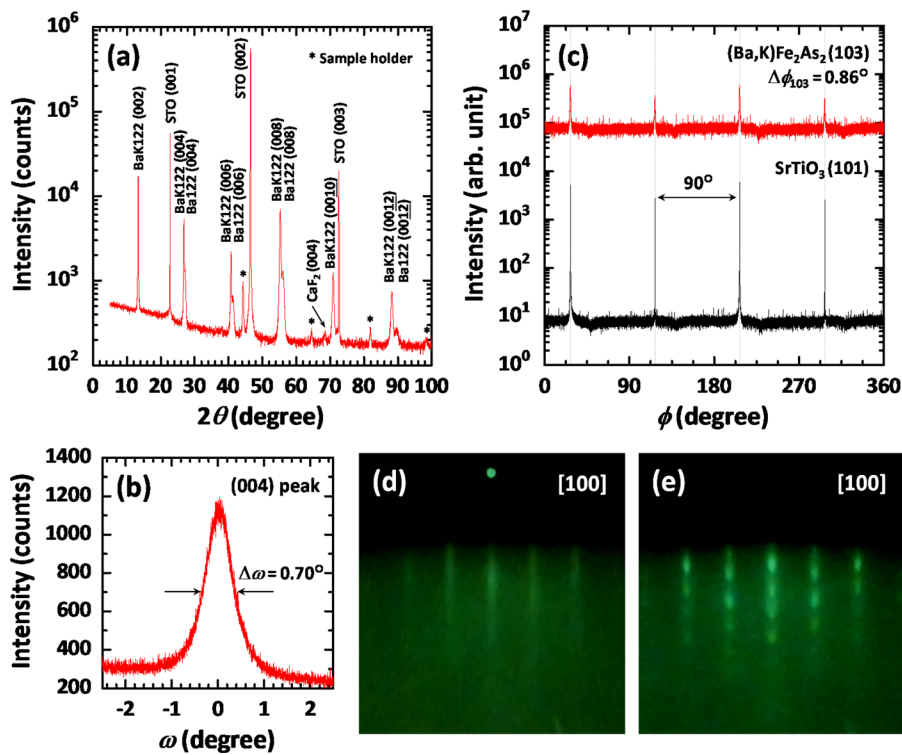


FIG. 1. (a) Out-of-plane XRD pattern of the $(\text{Ba,K})\text{Fe}_2\text{As}_2/\text{BaFe}_2\text{As}_2$ grown on single crystal $\text{SrTiO}_3(001)$ substrates. (b) Rocking curve for (004) reflection of $(\text{Ba,K})\text{Fe}_2\text{As}_2$. (c) Comparison of ϕ -scan of $(\text{Ba,K})\text{Fe}_2\text{As}_2$ (103) plane and SrTiO_3 (101) plane. (d) and (e) are RHEED patterns of the BaFe_2As_2 buffer layer and $(\text{Ba,K})\text{Fe}_2\text{As}_2$ layer, respectively. The RHEED images were taken during the deposition along with an incident electron beam parallel to the substrate [100] azimuth.

RHEED observation confirm that $(\text{Ba,K})\text{Fe}_2\text{As}_2/\text{BaFe}_2\text{As}_2$ is epitaxially grown on $\text{SrTiO}_3(001)$ substrates.

Epitaxial thin films of $(\text{Ba,K})\text{Fe}_2\text{As}_2$ were also prepared on [001]-tilt-type SrTiO_3 bicrystal substrates with θ_{GBS} up to 36.8° . **Figure 2(a)** shows the out-of-plane XRD pattern of the $(\text{Ba,K})\text{Fe}_2\text{As}_2/\text{BaFe}_2\text{As}_2$ prepared on SrTiO_3 bicrystal substrate with a θ_{GB} of 36.8° , which was deposited together with the sample shown in **Figs. 1(a)–1(c)**. Films prepared simultaneously on SrTiO_3 bicrystal substrates with $\theta_{\text{GB}} = 24^\circ$ and 30° are shown in the **supplementary material** (Fig. S5). The out-of-plane XRD pattern shown in **Fig. 2(a)** is identical to that shown in **Fig. 1(a)**, meaning that there is no difference in the out-of-plane alignment between the film on single crystal substrates and bicrystal substrates.

The c -axis length was 13.281\AA which is almost the same as that obtained for the film prepared on the single crystal substrate. **Figure 2(b)** shows the in-plane XRD pattern of the film and substrate. Both film and substrate show two sets of peaks with a 90° periodicity and a relative separation of 36.3° , implying tetragonal structures having a misorientation corresponding to the tilt angle of the SrTiO_3 bicrystal substrates. Eight sharp peaks were observed at the same angle for both the $(\text{Ba,K})\text{Fe}_2\text{As}_2$ (103) plane and the SrTiO_3 (101) plane, indicating a perfect transfer of the grain orientation from the bicrystal substrate (average θ_{GBS} of $(\text{Ba,K})\text{Fe}_2\text{As}_2$ and SrTiO_3 are 36.31° and 36.30° , respectively). The FWHM of the film ($\Delta\phi_{103} = 0.77^\circ$) is comparable to that of high-quality $\text{Ba}(\text{Fe},\text{Co})_2\text{As}_2$ epitaxial thin films prepared on bicrystal substrates.^{16,30}

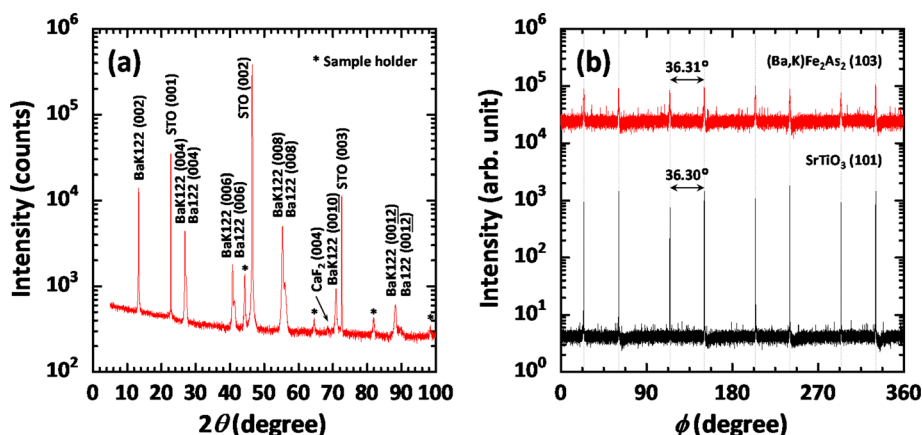


FIG. 2. (a) $2\theta/\omega$ -scan of $(\text{Ba,K})\text{Fe}_2\text{As}_2/\text{BaFe}_2\text{As}_2$ film deposited on a [001]-tilt-type SrTiO_3 bicrystal substrate with $\theta_{\text{GB}} = 36.8^\circ$. (b) Comparison of ϕ -scan of $(\text{Ba,K})\text{Fe}_2\text{As}_2$ (103) plane and SrTiO_3 (101) plane. The average θ_{GBS} of $(\text{Ba,K})\text{Fe}_2\text{As}_2$ and SrTiO_3 are 36.31° and 36.30° , respectively.

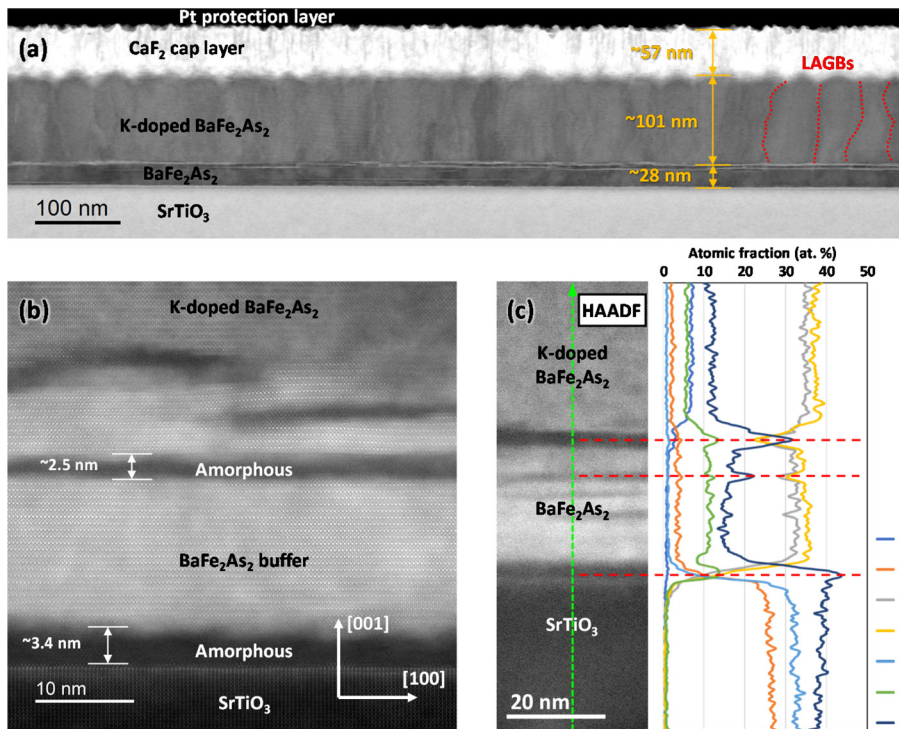


FIG. 3. Cross-sectional microstructural analysis of the (Ba,K)Fe₂As₂ film epitaxially grown on SrTiO₃ substrate. (a) The bright-field STEM image of the cross-sectional sample. On the right side of the image, few LAGBs are highlighted by red dashed lines. (b) Atomic-resolution HAADF-STEM image of the interfaces between (Ba,K)Fe₂As₂ and BaFe₂As₂ and SrTiO₃. (c) Line scanning of elemental analysis along the green dashed line in the left panel.

Figure 3(a) shows the bright-field STEM image of the (Ba,K)Fe₂As₂/BaFe₂As₂/SrTiO₃ film in the cross-sectional direction. As can be seen in the figure, the (Ba,K)Fe₂As₂ film shows a clear columnar bright and dark contrast, which implies that the film contains dense vertical low-angle grain boundaries (LAGB), similar to the (Ba,K)Fe₂As₂ film grown on a CaF₂ single-crystal substrate.⁶ The width between the LAGBs, which is indicated as red dashed lines in Fig. 3(a), is 50–80 nm. Many amorphous layers parallel to the *ab*-plane were found in the BaFe₂As₂ buffer, as shown in Fig. 3(a) and the atomic-resolution image, Fig. 3(b). Such defects were not found in the (Ba,K)Fe₂As₂ layer. The epitaxial relationship between the three layers can be clearly observed in Fig. 3(b) as (001)[100]-(Ba,K)Fe₂As₂ || (001)[100]-BaFe₂As₂ || (001)[100]-SrTiO₃. Therefore, it can be said that the BaFe₂As₂ layer can play the role of an effective buffer for the growth of a perfect (Ba,K)Fe₂As₂ superconducting film. In addition, with the help of the atomic-resolution images, the *c*-axis length of the (Ba,K)Fe₂As₂ layer was measured to be 13.237 Å with reference to the lattice parameter of SrTiO₃ (*a* = 3.905 Å), which is similar to that of XRD measurements. Figure 3(c) shows the elemental analysis along the green dashed line in the left panel, which shows that the potassium has been doped into the superconducting layer successfully. In addition, the right panel in Fig. 3(c) also shows clear barium peaks corresponding to the amorphous layers, which indicate that the active barium element is prone to segregate. This phenomenon is also observed in polycrystalline BaFe₂As₂ bulks.³¹ The excess O element in the (Ba,K)Fe₂As₂ layer and BaFe₂As₂ buffer is attributed to brief contact with the atmosphere during TEM sample preparation and observation.

Figure 4 shows the temperature dependence of resistivity of (Ba,K)Fe₂As₂ prepared on a [001]-tilt-type SrTiO₃ bicrystal substrate with $\theta_{GB} = 36.8^\circ$. Resistivity for both intergrain and intragrain was

measured as illustrated in the inset. The resistivity for intragrain and intergrain at 300 K was 344 and 319 $\mu\Omega$ cm, respectively, which is comparable to that of a single crystal ($\sim 310 \mu\Omega$ cm).³² The residual resistivity ratio (RRR) defined by $\rho(300\text{ K})/\rho(39\text{ K})$ was 6.00 for the intragrain transport, which is smaller than that of the high-quality single crystal (11.6)³² but comparable to the Ba_{0.64}K_{0.36}Fe₂As₂/BaFe₂As₂

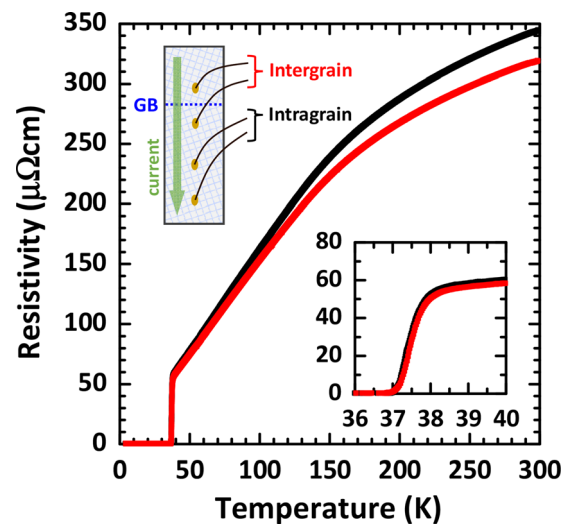


FIG. 4. Comparison of intragrain and intergrain resistivity for (Ba,K)Fe₂As₂/BaFe₂As₂ prepared on [001]-tilt-type SrTiO₃ bicrystal substrates with $\theta_{GB} = 36.8^\circ$. The inset is the schematic image of the measurement and the enlarged view near T_c .

film deposited on MgO substrates (5.8).²² As for the intergrain transport, the RRR was 5.73, comparable to the intragrain transport. Sharp superconducting transitions ($\Delta T_c = 0.77$ K) were observed at a high T_c of 38.0 K for both intragrain and intergrain transports. This high T_c is reasonable compared to $\text{Ba}_{0.6}\text{K}_{0.4}\text{Fe}_2\text{As}_2$ of a single crystal (~ 38 K) and polycrystal (~ 38 K).^{26,32,33} The unchanged ΔT_c for the intergrain transport indicates that there is no impurity phase at the AGB, which could cause the transition width to broaden. The unchanged T_c and ΔT_c are consistent with the high-quality AGB of $\text{Ba}(\text{Fe},\text{Co})_2\text{As}_2$ with $\theta_{\text{GB}} \sim 37.1^\circ$,¹⁶ thus indicating that the obtained AGB is of high quality.

Figure 5 shows the high-field J_c property of the film measured for $H//c$. The nominal composition of this film is $\text{Ba}_{0.63}\text{K}_{0.37}\text{Fe}_2\text{As}_2$, which is slightly lower than that of the sample shown in Figs. 1, 2, and 4. The film exhibits a very high J_c of 14.3 MA/cm² at 4.2 K, under the self-field. In addition, the J_c retains 1 MA/cm² even at 15 K and 16 T. This value is comparable to the J_c obtained by the film grown on CaF_2 substrate with LAGB networks.⁶ Moreover, the pinning force density (defined by the product of J_c and magnetic field) was 410 GN/m³ at 4.2 K and 16 T, which is the highest value ever reported among FBSs. The high J_c performance is most likely due to the flux pinning by the LAGBs observed in Fig. 3(a). The achievement of high J_c $(\text{Ba},\text{K})\text{Fe}_2\text{As}_2$ epitaxial thin films on SrTiO_3 substrates reveals the high potential of $(\text{Ba},\text{K})\text{Fe}_2\text{As}_2$ for applications and enables further high-field experiments in the form of epitaxial thin films.

The previously reported AGBs of $(\text{Ba},\text{K})\text{Fe}_2\text{As}_2$ prepared on MgO revealed a high grain boundary transparency of the $(\text{Ba},\text{K})\text{Fe}_2\text{As}_2$.²³ However, for some reason, $(\text{Ba},\text{K})\text{Fe}_2\text{As}_2$ films prepared on MgO bicrystal substrates were slightly distorted, and spontaneous structural deformations were observed around AGB. Therefore, the macroscopic θ_{GB} (determined from XRD) does not actually correspond to the microscopic θ_{GB} (observed from TEM). Compared with the previously reported AGBs on MgO substrates, AGBs prepared on SrTiO_3 substrates yield better crystallinity. Specifically, a high intensity

of out-of-plane diffraction peaks and a narrow FWHM for ϕ -scan of (103) plane. The improved crystallinity and the absence of 45°-rotated grains in the AGBs of $(\text{Ba},\text{K})\text{Fe}_2\text{As}_2$ provide the opportunity to study more intrinsic grain boundary properties. The results also prove that BaFe_2As_2 is an effective buffer layer for realizing films with high crystallinity. The achieved AGBs allow direct comparison with the grain boundary characteristics of $\text{Ba}(\text{Fe},\text{Co})_2\text{As}_2$ to observe the intrinsic grain boundary nature of the $(\text{Ba},\text{K})\text{Fe}_2\text{As}_2$ up to high θ_{GB} s of 36.8°. The physical properties of the $(\text{Ba},\text{K})\text{Fe}_2\text{As}_2$ AGBs will be reported in the next reports. In addition to the investigation of grain boundary nature, the high quality of the films such as high crystallinity, a small ΔT_c , and a large J_c can enable thin film device applications with Josephson junctions. Superconducting devices such as SQUID along the bicrystal grain boundary junction using $(\text{Ba},\text{K})\text{Fe}_2\text{As}_2$ epitaxial thin films prepared on SrTiO_3 bicrystal substrates may prove the potential as superconducting devices.

To conclude, $(\text{Ba},\text{K})\text{Fe}_2\text{As}_2$ epitaxial thin films were prepared on $\text{SrTiO}_3(001)$ substrates by implementing the BaFe_2As_2 buffer layer. The film exhibits a T_c of 38.0 K and a J_c exceeding 14 MA/cm² which implies the high quality of the film. The same growth procedure can be adopted to achieve high-angle AGBs of $(\text{Ba},\text{K})\text{Fe}_2\text{As}_2$ on bicrystal substrates. The intrinsic grain boundary nature of $(\text{Ba},\text{K})\text{Fe}_2\text{As}_2$ can be investigated with transport and magnetization measurements, and nano-structural observations. The insights that would be obtained from the AGBs of $(\text{Ba},\text{K})\text{Fe}_2\text{As}_2$ could foster the enhancement of transport J_c of the superconducting wires or coated conductors, trapped magnetic field of superconducting permanent magnets, and superconducting device applications of $(\text{Ba},\text{K})\text{Fe}_2\text{As}_2$.

See the [supplementary material](#) for the film growth on the pre-treated SrTiO_3 substrates, crystal structure and resistivity of BaFe_2As_2 and $(\text{Ba},\text{K})\text{Fe}_2\text{As}_2$ grown directly on SrTiO_3 substrates, detailed calculation process of the lattice parameter, detailed RHEED patterns during the growth, and $(\text{Ba},\text{K})\text{Fe}_2\text{As}_2$ epitaxial thin films grown on SrTiO_3 bicrystal substrates with $\theta_{\text{GB}} = 24^\circ$ and 30° .

This work was supported by the JST CREST Grant No. JPMJCR18J4 and the Grant-in-Aid for JSPS Fellows Grant No. JP22J23857. A portion of this work was performed at the National High Magnetic Field Laboratory, which is supported by the National Science Foundation Cooperative Agreement No. DMR-2128556 and the State of Florida. The research work at FSU was primarily funded by Grant No. DE-SC0018750 from the U.S. Department of Energy, Office of Science, Office of High Energy Physics.

AUTHOR DECLARATIONS

Conflict of Interest

The authors have no conflicts to disclose.

Author Contributions

Dongyi Qin: Funding acquisition (equal); Investigation (equal); Methodology (equal); Resources (lead); Writing – original draft (lead); Writing – review & editing (equal). **Zimeng Guo:** Investigation (equal); Methodology (equal); Writing – original draft (equal); Writing – review & editing (equal). **Chiara Tarantini:** Funding acquisition

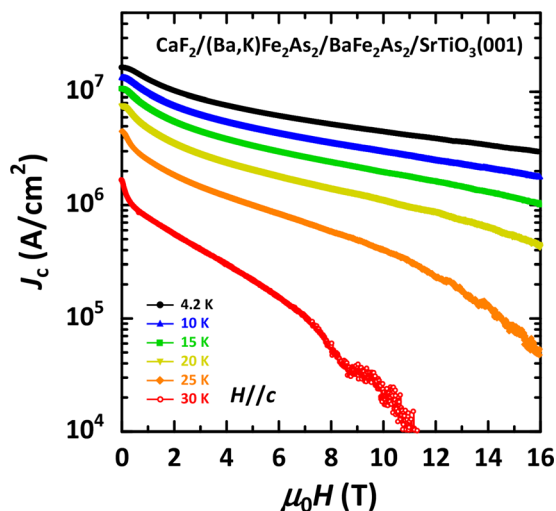


FIG. 5. J_c property for $(\text{Ba},\text{K})\text{Fe}_2\text{As}_2/\text{BaFe}_2\text{As}_2$ grown on single crystal $\text{SrTiO}_3(001)$ substrates. Fluctuations at high fields and high temperatures are due to the approaching of T_c .

(equal); Investigation (equal); Methodology (equal); Supervision (equal); Writing – review & editing (equal). **Satoshi Hata:** Methodology (equal); Supervision (equal); Writing – review & editing (equal). **Michio Naito:** Methodology (equal); Resources (equal); Writing – review & editing (equal). **Akiyasu Yamamoto:** Conceptualization (lead); Funding acquisition (lead); Investigation (equal); Methodology (equal); Resources (equal); Supervision (equal); Writing – review & editing (equal).

DATA AVAILABILITY

The data that support the findings of this study are available from the corresponding author upon reasonable request.

REFERENCES

- Y. Kamihara, T. Watanabe, M. Hirano, and H. Hosono, "Iron-based layered superconductor $\text{La}[\text{O}_{1-x}\text{F}_x]\text{FeAs}$ ($x = 0.05 - 0.12$) with $T_c = 26$ K," *J. Am. Chem. Soc.* **130**(11), 3296 (2008).
- H. Hosono, A. Yamamoto, H. Hiramatsu, and Y. Ma, "Recent advances in iron-based superconductors toward applications," *Mater. Today* **21**(3), 278 (2018).
- K. Kihou, T. Saito, K. Fujita, S. Ishida, M. Nakajima, K. Horigane, H. Fukazawa, Y. Kohori, S. Uchida, J. Akimitsu, A. Iyo, C. H. Lee, and H. Eisaki, "Single-crystal growth of $\text{Ba}_{1-x}\text{K}_x\text{Fe}_2\text{As}_2$ by KAs self-flux method," *J. Phys. Soc. Jpn.* **85**(3), 034718 (2016).
- M. Rotter, M. Tegel, and D. Johrendt, "Superconductivity at 38 K in the iron arsenide $(\text{Ba}_{1-x}\text{K}_x)\text{Fe}_2\text{As}_2$," *Phys. Rev. Lett.* **101**(10), 107006 (2008).
- C. Tarantini, A. Gurevich, J. Jaroszynski, F. Balakirev, E. Bellingeri, I. Pallecchi, C. Ferdeghini, B. Shen, H. H. Wen, and D. C. Larbalestier, "Significant enhancement of upper critical fields by doping and strain in iron-based superconductors," *Phys. Rev. B* **84**(18), 184522 (2011).
- K. Iida, D. Qin, C. Tarantini, T. Hatano, C. Wang, Z. Guo, H. Gao, H. Saito, S. Hata, M. Naito, and A. Yamamoto, "Approaching the ultimate superconducting properties of $(\text{Ba},\text{K})\text{Fe}_2\text{As}_2$ by naturally formed low-angle grain boundary networks," *NPG Asia Mater.* **13**(1), 68 (2021).
- A. Takahashi, S. Pyon, Y. Kobayashi, T. Kambara, A. Yoshida, S. Okayasu, A. Ichinose, and T. Tamegai, "Effects of splayed columnar defects on critical current density in $\text{CaKFe}_4\text{As}_4$," *J. Phys.* **1590**(1), 012015 (2020).
- H. Q. Yuan, J. Singleton, F. F. Balakirev, S. A. Baily, G. F. Chen, J. L. Luo, and N. L. Wang, "Nearly isotropic superconductivity in $(\text{Ba},\text{K})\text{Fe}_2\text{As}_2$," *Nature* **457**(7229), 565 (2009).
- S. Liu, C. Yao, H. Huang, C. Dong, W. Guo, Z. Cheng, Y. Zhu, S. Awaji, and Y. Ma, "High-performance $\text{Ba}_{1-x}\text{K}_x\text{Fe}_2\text{As}_2$ superconducting tapes with grain texture engineered via a scalable fabrication," *Sci. China Mater.* **64**(10), 2530 (2021).
- W. Guo, C. Yao, H. Huang, C. Dong, S. Liu, C. Wang, and Y. Ma, "Enhancement of transport J_c in $(\text{Ba}, \text{K})\text{Fe}_2\text{As}_2$ HIP processed round wires," *Supercond. Sci. Technol.* **34**(9), 094001 (2021).
- X. Zhang and Y. Ma, "Progress in the development of the 122-type IBS wires," *Superconductivity* **2**, 100010 (2022).
- P. Yang, D. Wang, C. Yao, W. Guo, H. Huang, M. Han, C. Tu, F. Liu, D. Jiang, and Y. Ma, "Superior transport current densities in $(\text{Ba}, \text{K})\text{Fe}_2\text{As}_2$ superconducting tapes realized by combined strengthening of grain texture and flux pinning," *J. Alloys Compd.* **1000**, 175081 (2024).
- C. Dong, Q. Xu, and Y. Ma, "Towards high-field applications: High-performance, low-cost iron-based superconductors," *Natl. Sci. Rev.* **11**, nwae122 (2024).
- A. Yamamoto, S. Tokuta, A. Ishii, A. Yamanaka, Y. Shimada, and M. D. Ainslie, "Superstrength permanent magnets with iron-based superconductors by data- and researcher-driven process design," *NPG Asia Mater.* **16**(1), 29 (2024).
- T. Katase, Y. Ishimaru, A. Tsukamoto, H. Hiramatsu, T. Kamiya, K. Tanabe, and H. Hosono, "Advantageous grain boundaries in iron pnictide superconductors," *Nat. Commun.* **2**(1), 409 (2011).
- K. Iida, S. Haindl, F. Kurth, J. Hänisch, L. Schulz, and B. Holzapfel, "BaFe₂As₂/Fe bilayers with [001]-tilt grain boundary on MgO and SrTiO₃ bicrystal substrates," *Phys. Procedia* **45**, 189 (2013).
- S. Lee, J. Jiang, J. D. Weiss, C. M. Folkman, C. W. Bark, C. Tarantini, A. Xu, D. Abrahimov, A. Polyanskii, C. T. Nelson, Y. Zhang, S. H. Baek, H. W. Jang, A. Yamamoto, F. Kametani, X. Q. Pan, E. E. Hellstrom, A. Gurevich, C. B. Eom, and D. C. Larbalestier, "Weak-link behavior of grain boundaries in superconducting $\text{Ba}(\text{Fe}_{1-x}\text{Co}_x)_2\text{As}_2$ bicrystals," *Appl. Phys. Lett.* **95**(21), 212505 (2009).
- A. Sakagami, T. Kawaguchi, M. Tabuchi, T. Ujihara, Y. Takeda, and H. Ikuta, "Critical current density and grain boundary property of $\text{BaFe}_2(\text{As},\text{P})_2$ thin films," *Physica C* **494**, 181 (2013).
- K. Iida, T. Omura, T. Matsumoto, T. Hatano, and H. Ikuta, "Grain boundary characteristics of oxypnictide $\text{NdFeAs}(\text{O},\text{F})$ superconductors," *Supercond. Sci. Technol.* **32**(7), 074003 (2019).
- W. Si, C. Zhang, X. Shi, T. Ozaki, J. Jaroszynski, and Q. Li, "Grain boundary junctions of $\text{FeSe}_{0.5}\text{Te}_{0.5}$ thin films on SrTiO₃ bi-crystal substrates," *Appl. Phys. Lett.* **106**(3), 032602 (2015).
- D. Qin, K. Iida, T. Hatano, H. Saito, Y. Ma, C. Wang, S. Hata, M. Naito, and A. Yamamoto, "Realization of epitaxial thin films of the superconductor K-doped BaFe_2As_2 ," *Phys. Rev. Mater.* **5**(1), 014801 (2021).
- D. Qin, K. Iida, Z. Guo, C. Wang, H. Saito, S. Hata, M. Naito, and A. Yamamoto, "K-doped $\text{Ba}122$ epitaxial thin film on MgO substrate by buffer engineering," *Supercond. Sci. Technol.* **35**(9), 09LT01 (2022).
- T. Hatano, D. Qin, K. Iida, H. Gao, Z. Guo, H. Saito, S. Hata, Y. Shimada, M. Naito, and A. Yamamoto, "High tolerance of the superconducting current to the large grain boundary angles in potassium-doped BaFe_2As_2 ," *NPG Asia Mater.* **16**(1), 41 (2024).
- S. Lee, J. Jiang, Y. Zhang, C. W. Bark, J. D. Weiss, C. Tarantini, C. T. Nelson, H. W. Jang, C. M. Folkman, S. H. Baek, A. Polyanskii, D. Abrahimov, A. Yamamoto, J. W. Park, X. Q. Pan, E. E. Hellstrom, D. C. Larbalestier, and C. B. Eom, "Template engineering of Co-doped BaFe_2As_2 single-crystal thin films," *Nat. Mater.* **9**(5), 397 (2010).
- M. Sakoda, K. Iida, and M. Naito, "Recent progress in thin-film growth of Fe-based superconductors: Superior superconductivity achieved by thin films," *Supercond. Sci. Technol.* **31**(9), 093001 (2018).
- M. Rotter, M. Pangerl, M. Tegel, and D. Johrendt, "Superconductivity and crystal structures of $(\text{Ba}_{1-x}\text{K}_x)\text{Fe}_2\text{As}_2$ ($x = 0 - 1$)," *Angew. Chem., Int. Ed.* **47**(41), 7949 (2008).
- M. Kawasaki, K. Takahashi, T. Maeda, R. Tsuchiya, M. Shinohara, O. Ishiyama, T. Yonezawa, M. Yoshimoto, and H. Koinuma, "Atomic control of the SrTiO₃ crystal surface," *Science* **266**(5190), 1540 (1994).
- J. Peng, C. S. Hao, H. Y. Liu, and Y. Yan, "Two-step treatment to obtain single-terminated SrTiO₃ substrate and the related difference in both LaAlO_3 film growth and electronic property," *AIP Adv.* **11**(8), 085303 (2021).
- C. P. Bean, "Magnetization of high-field superconductors," *Rev. Mod. Phys.* **36**(1), 31 (1964).
- T. Katase, H. Hiramatsu, T. Kamiya, and H. Hosono, "High critical current density 4 MA/cm² in Co-doped BaFe_2As_2 epitaxial films grown on $(\text{La},\text{Sr})(\text{Al},\text{Ta})\text{O}_3$ substrates without buffer layers," *Appl. Phys. Express* **3**(6), 063101 (2010).
- Z. Guo, K. Muraoka, H. Gao, Y. Shimada, T. Harada, S. Tokuta, Y. Hasegawa, A. Yamamoto, and S. Hata, "Planar defects and strain distributions in polycrystalline BaFe_2As_2 superconductors synthesized by mechanochemical methods," *Acta Mater.* **266**, 119648 (2024).
- M. Nakajima, S. Ishida, T. Tanaka, K. Kihou, Y. Tomioka, T. Saito, C. H. Lee, H. Fukazawa, Y. Kohori, T. Kakeshita, A. Iyo, T. Ito, H. Eisaki, and S. Uchida, "Normal-state charge dynamics in doped BaFe_2As_2 : Roles of doping and necessary ingredients for superconductivity," *Sci. Rep.* **4**(1), 5873 (2014).
- Y. Liu, M. A. Tanatar, W. E. Straszheim, B. Jensen, K. W. Dennis, R. W. McCallum, V. G. Kogan, R. Prozorov, and T. A. Lograsso, "Comprehensive scenario for single-crystal growth and doping dependence of resistivity and anisotropic upper critical fields in $(\text{Ba}_{1-x}\text{K}_x)\text{Fe}_2\text{As}_2$ ($0.22 \leq x \leq 1$)," *Phys. Rev. B* **89**(13), 134504 (2014).